NanoImpact 28 (2022) 100439

Contents lists available at ScienceDirect

NanoImpact

journal homepage: www.elsevier.com/locate/nanoimpact

An inter-laboratory effort to harmonize the cell-delivered in vitro dose of aerosolized materials

Anne Bannuscher [a,1], Otmar Schmid [b,c,1], Barbara Drasler [a], Alain Rohrbasser [a], Hedwig M. Braakhuis [d], Kirsty Meldrum [e], Edwin P. Zwart [d], Eric R. Gremmer [d], Barbara Birk [f], Manuel Rissel [f], Robert Landsiedel [f,g], Elisa Moschini [h], Stephen J. Evans [e], Pramod Kumar [b,c], Sezer Orak [b,c], Ali Doryab [b,c], Johanna Samulin Erdem [i], Tommaso Serchi [h], Rob J. Vandebriel [d], Flemming R. Cassee [d,j], Shareen H. Doak [e], Alke Petri-Fink [a], Shanbeh Zienolddiny [i], Martin J. D. Clift [e], Barbara Rothen-Rutishauser [a,*]

[a] Adolphe Merkle Institute, University of Fribourg, Chemin des Verdiers 4, 1700 Fribourg, Switzerland
[b] Comprehensive Pneumology Center (CPC-M), Helmholtz Zentrum München - Member of the German Center for Lung Research (DZL), Max-Lebsche-Platz 31, 81377 Munich, Germany
[c] Institute of Lung Health and Immunity, Helmholtz Zentrum München – German Research Center for Environmental Health, 85764 Neuherberg, Germany
[d] National Institute for Public Health and the Environment (RIVM), PO Box 1, 3720, BA, Bilthoven, the Netherlands
[e] In Vitro Toxicology Group, Faculty of Medicine, Health and Life Sciences, Medical School, Institute of Life Sciences, Centre for NanoHealth, Swansea University, Singleton Campus, Wales SA2 8PP, UK
[f] BASF SE, Experimental Toxicology and Ecology, 67056 Ludwigshafen am Rhein, Germany
[g] Free University of Berlin, Pharmacy, Pharmacology and Toxicology, 14195 Berlin, Germany.
[h] Department of Environmental Research and Innovation, Luxembourg Institute of Science and Technology (LIST), 41 rue du Brill, L4422 Belvaux, Grand-Duchy of Luxembourg, Luxembourg
[i] National Institute of Occupational Health (STAMI), N-0033 Oslo, Norway
[j] Institute for Risk Assessment Sciences, Utrecht University, Utrecht, the Netherlands

ARTICLE INFO

Keywords:
Aerosol-cell exposure
Nanoparticles
Nanomaterials
Inter-laboratory comparison
Standard operating procedure (SOP)
VITROCELL® Cloud12 system
DQ_{12}
TiO_2 NM-105

ABSTRACT

Air-liquid interface (ALI) lung cell models cultured on permeable transwell inserts are increasingly used for respiratory hazard assessment requiring controlled aerosolization and deposition of any material on ALI cells. The approach presented herein aimed to assess the transwell insert-delivered dose of aerosolized materials using the VITROCELL® Cloud12 system, a commercially available aerosol-cell exposure system. An inter-laboratory comparison study was conducted with seven European partners having different levels of experience with the VITROCELL® Cloud12. A standard operating procedure (SOP) was developed and applied by all partners for aerosolized delivery of materials, *i.e.,* a water-soluble molecular substance (fluorescence-spiked salt) and two poorly soluble particles, crystalline silica quartz (DQ_{12}) and titanium dioxide nanoparticles (TiO_2 NM-105). The material dose delivered to transwell inserts was quantified with spectrofluorometry (fluorescein) and with the quartz crystal microbalance (QCM) integrated in the VITROCELL® Cloud12 system. The shape and agglomeration state of the deposited particles were confirmed with transmission electron microscopy (TEM).

Inter-laboratory comparison of the device-specific performance was conducted in two steps, first for molecular substances (fluorescein-spiked salt), and then for particles. Device- and/or handling-specific differences in aerosol deposition of VITROCELL® Cloud12 systems were characterized in terms of the so-called deposition factor (DF), which allows for prediction of the transwell insert-deposited particle dose from the particle concentration in the aerosolized suspension. Albeit DF varied between the different labs from 0.39 to 0.87 (mean

Abbreviations: ALI, air-liquid interface; ALICE, air-liquid interface cell exposure; BSA, bovine serum albumin; CV, coefficient of variation; DQ_{12}, crystalline silica quartz; DF, deposition factor; DPBS, dulbecco's phosphate buffered saline; DLS, dynamic light scattering; FCS, fetal calf serum; QCM, quartz crystal microbalance; SD, standard deviation; SEM, standard error mean; SOP, standard operating procedure; TiO_2 NM-105, titanium dioxide nanoparticles; TEM, transmission electron microscopy.

* Corresponding author at: Adolphe Merkle Institute, Chemin des Verdiers 4, CH-1700 Fribourg, Switzerland.
E-mail address: barbara.rothen@unifr.ch (B. Rothen-Rutishauser).

[1] Authors contributed equally.

https://doi.org/10.1016/j.impact.2022.100439
Received 19 August 2022; Received in revised form 13 November 2022; Accepted 14 November 2022
Available online 17 November 2022

(coefficient of variation (CV)): 0.64 (28%)), the QCM of each VITROCELL® Cloud 12 system accurately measured the respective transwell insert-deposited dose. Aerosolized delivery of DQ_{12} and TiO_2 NM-105 particles showed good linearity ($R^2 > 0.95$) between particle concentration of the aerosolized suspension and QCM-determined insert-delivered particle dose. The VITROCELL® Cloud 12 performance for DQ_{12} particles was identical to that for fluorescein-spiked salt, *i.e.*, the ratio of measured and salt-predicted dose was 1.0 (29%). On the other hand, a *ca.* 2-fold reduced dose was observed for TiO_2 NM-105 (0.54 (41%)), which was likely due to partial retention of TiO_2 NM-105 agglomerates in the vibrating mesh nebulizer of the VITROCELL® Cloud12.

This inter-laboratory comparison demonstrates that the QCM integrated in the VITROCELL® Cloud 12 is a reliable tool for dosimetry, which accounts for potential variations of the transwell insert-delivered dose due to device-, handling- and/or material-specific effects. With the detailed protocol presented herein, all seven partner laboratories were able to demonstrate dose-controlled aerosolization of material suspensions using the VITROCELL® Cloud12 exposure system at dose levels relevant for observing *in vitro* hazard responses. This is an important step towards regulatory approved implementation of ALI lung cell cultures for *in vitro* hazard assessment of aerosolized materials.

1. Introduction

Inhalation as a route of exposure to aerosolized materials is of major concern and, thus, of great importance to hazard studies even at an early stage of material including nanomaterial development. Therefore, there is an imperative need of extensive research for realistic and reliable *in vitro* approaches with regard to assessing the hazards of aerosols. To mimic the inhalation of aerosols more adequately, lung cells can be cultured under air-liquid interface (ALI) conditions instead of being cultivated under submerged conditions (Voisin et al., 1977). The advantages of using this approach include direct delivery of the aerosolized materials to the surface of the lung cells mimicking *in vivo* conditions of inhalation (Paur et al., 2011; Lenz et al., 2014; Hiemstra et al., 2018; Lacroix et al., 2018; Upadhyay and Palmberg, 2018) and the availability of real-time methods for cell-delivered dosimetry, *e.g.*, by a quartz crystal microbalance (QCM) (Lenz et al., 2009; Schmid and Cassee, 2017; Ding et al., 2020). Materials including poorly soluble particles can be aerosolized directly as dry powder or as liquid avoiding the formation of a non-physiologic protein corona on the particles as it is observed under submerged cell culture conditions especially in the presence of bovine serum albumin (BSA) or fetal calf serum (FCS) (Paur et al., 2011; Limbach et al., 2005; Lynch et al., 2007). Moreover, the inhalation of particles without a protein corona mirrors the real-world situation, whereby a protein corona is only formed upon contact with the protein-rich lung fluid (Wohlleben et al., 2016).

Numerous ALI aerosol-cell exposure devices have been developed that vary greatly in methodology and performance parameters. These methods can be distinguished based on their mechanism for aerosol deposition on the cells. While earlier approaches relied on aerosol diffusion and sedimentation (Upadhyay and Palmberg, 2018; Aufderheide and Mohr, 2000; Bitterle et al., 2006), electrostatically and thermophoretically enhanced aerosol deposition can improve the delivery efficiency and rate of deposition and hence reduce the required aerosol-cell exposure times for reaching biologically relevant target doses (Savi et al., 2008; de Bruijne et al., 2009; Ritter et al., 2020). For even higher aerosol deposition rates and material delivery efficiency, cloud-enhanced gravitational settling was introduced leveraging the settling speed of a dense cloud of particles as compared to single-aerosol deposition (Lenz et al., 2014; Lenz et al., 2009). More details on these and other methods of aerosolized substance delivery to ALI lung cell culture models can be found elsewhere (Paur et al., 2011; Ehrmann et al., 2020). Most of these aerosol-cell exposure systems are neither commercially available nor widely used. Notable exceptions include the PreciseInhale system (Inhalation Sciences, Sweden) and the VITROCELL® Cloud technology. The former utilizes a focused high-pressure air pulse (DustGun) or a vibrating mesh nebulizer to disperse dry powder or liquid droplets into a holding chamber from which aerosol is withdrawn via a defined air flow to a stagnation point flow system for diffusion- and sedimentation-based aerosol-cell deposition. This method has been employed to study for instance the oxidative potential and macrophage polarization of diesel exhaust soot (Ji et al., 2018). Alternatively, the air-liquid interface cell exposure (ALICE) Cloud device (Lenz et al., 2014) aerosolizes aqueous material suspensions with a vibrating mesh nebulizer directly into an exposure system leveraging cloud-enhanced aerosol deposition. This technology has been made commercially available as the VITROCELL® Cloud system by VITROCELL® Systems (Germany). This system has been relatively widely used for *e.g.* nanomaterial hazard, particokinetics and drug efficacy investigations with water-soluble substances and poorly-soluble (nano-)particles and nanofibres (Lenz et al., 2014; Ding et al., 2020; Endes et al., 2014; Schmid et al., 2017; Barosova et al., 2020; Doryab et al., 2021).

Inter-laboratory studies are essential towards implementation of ALI cultures for *in vitro* hazard assessment of materials. In addition, both the robustness and reproducibility of a method needs to be demonstrated for regulatory acceptance (Hartung et al., 2004; Bas et al., 2021). An important expected outcome of such an inter-laboratory comparison study is a standardized operating procedure (SOP) for a specific method which is necessary to ensure globally harmonized *in vitro* testing approaches and should be in line with the guidance document on "good *in vitro* method practices" (GIVIMP) released by the OECD (OECD, 2018; Petersen et al., 2021). An SOP contains all information required to perform an alternative test including an itemized list of employed materials and devices, detailed instructions on experimental procedures to follow, positive and negative controls, as well as performance criteria (Elberskirch et al., 2022; Barosova et al., 2021). Such detailed information is key to harmonizing testing procedures, assuring data quality and confirming reproducibility of data and results obtained with the same method used by different personnel in different laboratories. The reliability of SOPs benefits from the input provided by a relatively large number of people which are typically involved in inter-laboratory comparison efforts (Xia et al., 2013; Elliott et al., 2017).

Here, we describe an inter-laboratory comparison study for material aerosol exposure and deposition measurements. For this purpose, the VITROCELL® Cloud12 system (VITROCELL Systems GmbH, Germany) was chosen since it combines advantages like ease-of-use and real-time dosimetry with a QCM, commercial availability and its relatively widespread use and routine operation in several laboratories (Ding et al., 2020; Fizeşan et al., 2019). This inter-laboratory effort aimed to compare the transwell insert-deposited dose of selected materials in the test system. We leveraged a fluorescein assay to characterize each VITROCELL® Cloud12 system for its deposition factor (DF), from which the cell-deposited dose and deposition efficiency can be predicted (Ding et al., 2020). We also provide a SOP for the aerosolization of two types of materials, namely crystalline silica DQ_{12} (Dörntruper silica quartz) particles and TiO_2 nanoparticles (NM-105). The materials have been both widely used for *in vitro* hazard testing (Arts et al., 2016; Wiemann et al., 2016) and categorized as toxicologically "active" in the DF4Grouping scheme introduced by the ECETOC in 2015 (Arts et al., 2016; Arts et al., 2015) qualifying them as materials to establish reactive lung cell models.

2. Material and methods

2.1. Materials

All chemicals, reagents, and materials used were purchased from Sigma-Aldrich except otherwise noted. DQ_{12} was received from the IOM (Institute of Occupational Medicine, UK), and TiO_2 NM-105 (Aeroxide®P25 by Evonik) was provided by the Fraunhofer Institute for Molecular Biology and Applied Ecology (Fraunhofer IME, Germany) (Table 1).

2.2. Preparation and characterization of particle suspension

Particles were dispersed according to the Nanogenotox protocol for toxicity testing (https://www.anses.fr/en/system/files/nanogenotox_deliverable_5.pdf) with slight modifications. The suspensions were prepared in a volume range between 4 mL and 10 mL of ultrapure water without BSA (with BSA in the original Nanogenotox protocol) in order to avoid formation of a non-physiologic protein corona and potential protein-induced foaming and/or (partial) clogging of the nebulizer which could compromise the particle-induced biological response and reproducibility of the particle deposition. Briefly, a target mass of 10.24 mg of the material in powder form was weighed into glass vials, pre-wetted with 20 µL ethanol for mitigation of particle hydrophobicity enabling a highly dispersed state of particles, and mixed with water to obtain a stock concentration of 2.56 mg/mL. The suspension was sonicated using an ultrasonic tip device delivering a total acoustic energy of 7056 +/− 103 J (mean ± SD) as described in the "*NANoREG SOP for probe-sonicator calibration of delivered acoustic power and de-agglomeration efficiency for in vitro and in vivo toxicological testing*" (Booth and Jensen, n. d.). The laboratories have used different sonicators, but all have adjusted the sonication process to reach the targeted total acoustic energy of 7056 +/− 103 J using this protocol. During the sonication process the samples were kept on ice to prevent overheating caused by the sonication device. The sample stocks were further diluted to 1 mg/mL suspensions. The working concentrations ranging from 125 to 500 µg/mL were prepared from those stocks. All suspensions were sonicated for 10 min in an ultrasonic bath and gently vortexed prior to usage.

2.3. Dynamic light scattering measurements

The hydrodynamic radius of TiO_2 and DQ_{12} particles in Milli-Q were recorded with a dynamic light scattering (DLS) spectrometer (LS Instruments AG, Fribourg, Switzerland) at the scattering angle of 50° and laser wavelength 660 nm. To calculate dimensions of TiO_2 and DQ_{12} particles, the obtained correlation functions. The polydispersity index and ζ-potential were determined by dynamic light scattering and phase-amplitude light scattering (ZetaPALS) in Milli-Q water (Brookhaven 90Plus Particle Size Analyzer, Brookhaven Instruments Corp., Holtsville, NY, USA), respectively. Five DLS and zeta potential measurements were recorded for each sample to estimate the mean and the standard deviation. The measurements TiO_2 and DQ_{12} particles were performed at a concentration of 125 µg/mL after sonication.

2.4. Inter-laboratory testing approach

The inter-laboratory testing approach was performed with consideration of the SOP developed within the H2020 project PATROLS. This *PATROLS SOP - Guidance Document for DQ_{12} and TiO_2 Aerosolization using VITROCELL® Cloud System* (https://patrols-h2020.eu/publications/sops/SOP-library-pdfs/3601_2_SOP_PATROLS_Cloud_Aerosolization.pdf?m=1669206589&) is henceforth referred to as PATROLS SOP. It was carried out by seven different participants: 1.) Adolphe Merkle Institute (AMI), Switzerland, 2.) National Institute for Public Health and the Environment (RIVM), The Netherlands, 3.) Swansea University Medical School (SU), United Kingdom, 4.) BASF SE, Experimental Toxicology and Ecology, Germany, 5.) Luxembourg Institute of Science and Technology (LIST), Luxemburg, 6.) Helmholtz Zentrum München - German Research Center for Environmental Health (HMGU), Germany and 7.) National Institute of Occupational Health (STAMI), Norway. Participants 1–4 were members of the PATROLS project, while partners 5–7 were external collaborators.

All partners used a VITROCELL® Cloud12 device (VITROCELL® Systems GmbH, Germany) (Fig. 1A) equipped with an Aeroneb® Lab nebulizer (4–6 µm pore size, Aerogen, Ireland) and a VITROCELL® QCM12. Technical details on the principle and setup of the QCM, the VITROCELL® Cloud12 system, and on nebulization of materials can be found in the PATROLS SOP and in Ding *et al.* (Ding et al., 2020).

2.5. Aerosolization of materials

The VITROCELL® Cloud12 system was heated up to 37 °C before use with the cover (exposure top) in place (Fig. 1A). Meanwhile, 250 µL of particle suspension or water (blank) was spiked with 2.5 µL of an isotonic NaCl solution (i.e., 0.009% *w/v* = 90 µg/mL NaCl was added to the particle suspension), since a small amount of ions are required for stable operation of the vibrating mesh nebulizer. After the transwell inserts were put in place, the QCM data acquisition was started and the QCM stability (at zero point) was measured for 1 min. Then, 200 µL of the freshly NaCl-spiked particle suspension (water) was used for nebulization. The acceptable time range for nebulizing 200 µL of water/suspension is

between 15 and 60 s (0.2–0.8 mL/min). After another 6 min (at 7 min), the cover (exposure top) of the chamber was lifted allowing the deposited sample on the QCM to dry for 1 min. Subsequently, the cover was put back on the VITROCELL® Cloud system to prevent artefacts in the QCM signal due to ventilation and temperature effects (see results for more details). The QCM data acquisition was stopped after another 3 min and the mean of the last 30 s of QCM data was considered the QCM readout of the cell-delivered dose. For cleaning between consecutive exposure runs, the reservoir of the nebulizer was rinsed with water prior to each usage. The deposition of water spiked with NaCl (0.009% *w/v*) was additionally measured for blank correction prior to each exposure. An overview of the aerosolization procedure and the observed QCM

Table 1
Overview of DQ_{12} and TiO_2 NM-105 characterization.

Material	Name	Composition/Structure	Primary Particle Size	Surface Area (BET)	Hydrodynamic Diameter D50 (water)	Zeta potential (pH 7.4)
			[nm]	[m^2/g]	[nm]	[mV]
Quartz CAS 14808–60-7	DQ_{12}	Quartz, 87% crystalline and 13% amorphous SiO_2^+	≤5 µm*	7.4*	305	−34.89
Titanium dioxide CAS 13463–67-7	TiO_2 NM-105	85% anatase and 15% rutile	21**	51**	1038	32.34

Data from the following references: * (Robock, 1973), ** (Karkossa et al., 2019). The hydrodynamic diameter and zeta potential were determined by AMI.

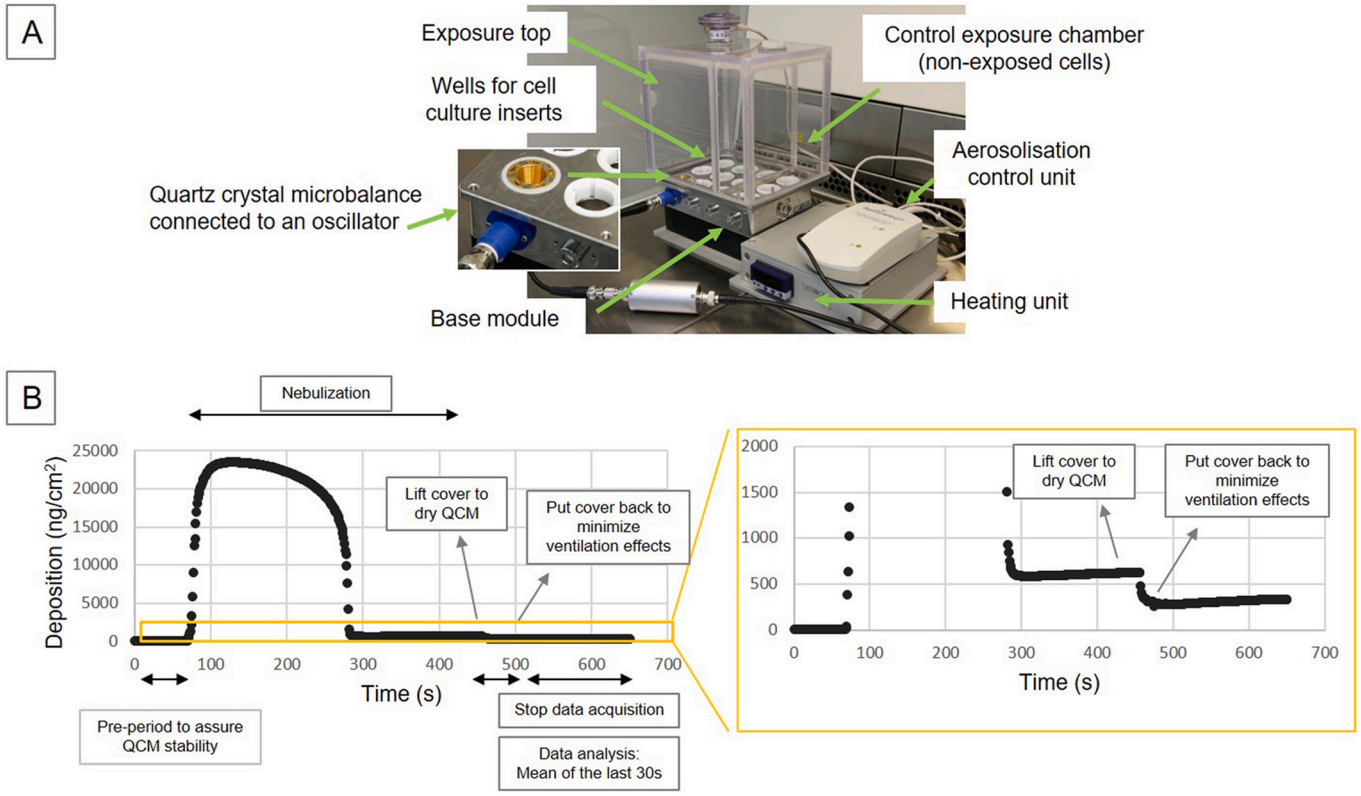

Fig. 1. The VITROCELL® Cloud12 system and QCM signal. A: The Cloud system in partner laboratory 1 (AMI). B: Overview of an aerosolization procedure and a typical QCM signal during an aerosolization experiment (here: 500 µg/mL DQ_{12}). The sudden drop at the end of the measurement (at *ca.* 420 s), right panel) indicates complete removal of water (drying) from the sample on the QCM as prerequisite for the QCM to provide accurate mass values. All values prior to this step-change in QCM signal (drying) cannot be interpreted in terms of mass due to biases of the QCM associated with residual water-induced viscoelastic effects of the QCM-deposited liquid.

response is given in Fig. 1B, and further details are given in the PATROLS SOP (https://patrols-h2020.eu/publications/sops/SOP-library-pdfs/3601_2_SOP_PATROLS_Cloud_Aerosolization.pdf?m=1669206589&).

2.6. Fluorescein assay for deposition factor (DF)

The fluorescein assay was used to determine the DF of the VITROCELL® Cloud12 which allows prediction of the transwell insert-delivered material dose. In addition, with this assay we were able to compare the material deposition on the transwell inserts and the corresponding QCM measurement.

The fluorescein assay was performed by each partner following the guidance document from VITROCELL® Systems (The document is available for VITROCELL® customers. Contact: support@vitrocell.com). Briefly, the VITROCELL® Cloud12 system equipped with a QCM was heated to 37 °C and the wells were filled with 3 mL distilled water except for the well, which was occupied with the QCM. It is important to note that this amount of liquid fills the wells without providing contact with the membrane of the transwell insert since this could bias the fluorescein assay. Some partners reduced this amount of water to 2.8 mL to safely prevent contact between water in transwell inserts. One partner (BASF) used stainless steel transwell inserts without a porous membrane (BASF) provided by VITROCELL® Systems. A 10.58 mg/mL fluorescein-spiked Dulbecco's Phosphate Buffered Saline (fluo-DPBS) solution was prepared consisting of 15 µg/mL fluorescein sodium salt (CAS 518–47-8) in DPBS (DPBS Gibco, 14,190,144) containing 10.56 mg/mL DPBS salt) and stored in the dark to prevent bleaching of the fluorescein dye. The 12-well transwell inserts (0.4 µm pore size, Corning, 3460) or stainless steel 12-well inserts without membrane manufactured by VITROCELL® Systems (BASF) were placed in the wells and 300 µL DPBS was added apically to collect the aerosolized fluorescein solution where the cells are typically located. Then, the fluo-DPBS (200 µL of stock solution) nebulization was performed in the same way as the (nano-)material suspensions were aerosolized and the QCM signal was recorded and analyzed as described above (Fig. 1B). Afterwards, an aliquot of 200 µL was taken out of each transwell insert, transferred into an Eppendorf tube, and diluted with 200 µL DPBS. The fluo-DPBS deposited on the quartz of the QCM was also collected by washing the quartz by pipetting 300 µL of DPBS onto the quartz, convectively mixing it by pipetting the liquid repeatedly up and down into and out of a pipette tip and finally withdrawing close to 300 µL DPBS (as much as possible) from the QCM again. From this, 200 µL were transferred into an Eppendorf tube and diluted with 200 µL DPBS. The 1:1 (2-fold) diluted liquids collected from the inserts and the QCM were pipetted into 96-well plates (Corning, flat bottom, black 96-well multiwell plates, CLS3603), the fluorescence intensity was measured (excitation/emission: 483/525 nm) and the fluorescein concentration was determined from the standard curve.

The primary outcome of the fluorescein assay is the DF of the Cloud system (fractional fluo-salt (here: fluo-DPBS) or aerosolized solute/particle dose reaching the bottom of the exposure chamber), which can be calculated from the measured fluorescein-induced fluorescence intensities of the liquids collected from the inserts and the QCM according to the following equations provided by Ding et al. (Ding et al., 2020). The DF normalizes the fluo-DPBS dose in the inserts to the theoretically possible maximum value assuming that all of the aerosolized fluo-DPBS dose is (uniformly) deposited on the bottom of the exposure chamber on the transwell inserts:

$$DF_{insert} = \frac{dep_{meas.insert}}{dep_{max}} = \frac{c_{insert} V_{insert}}{c_{neb} V_{neb} \frac{A_{insert}}{A_{chamber}}} \quad (1)$$

$$DF_{QCM} = \frac{dep_{meas.QCM}}{dep_{max}} = \frac{c_{QCM} V_{QCM}}{c_{neb} V_{neb} \frac{A_{QCM}}{A_{chamber}}} \quad (2)$$

DF_{insert}, DF_{QCM}: deposition factor measured in inserts (average of all eight inserts) and in QCM, respectively.

$dep_{meas.insert}$, $dep_{meas.QCM}$: deposited fluorescein mass per area (deposition) in inserts and on QCM measured by spectrofluorometry, respectively (μg/cm^2).

dep_{max}: maximum possible fluroescein deposition assuming that all of the fluorescein mass in the nebulizer deposits uniformly on the bottom of the exposure chamber, i.e., there is no loss of fluorescein (μg/cm^2).

c_{insert}, c_{QCM}: fluorescein concentration (μg/mL) in liquid retrieved from inserts or QCM, respectively, determined by spectrofluorometry (note: 2-fold dilution of samples was taken into account).

V_{insert}, V_{QCM}: volume of DPBS solution pre-filled into the inserts for collection of fluorescein (0.2 mL) or used for wash-off of fluorescein from QCM (0.3 mL).

c_{neb}, V_{neb}: concentration (15 μg/mL) and volume (0.2 mL) of nebulized fluorescein solution.

A_{insert}: area of insert available for (vertical) aerosol deposition (and cell seeding) (1.12 cm^2).

A_{QCM}: surface area of quartz crystal of QCM available for (vertical) aerosol deposition (1.04 cm^2).

$A_{chamber}$: total surface area at the bottom of the exposure chamber (141.6 cm^2).

In this study, the conversion of the fluorescence intensities in corresponding DF values was performed with the Excel sheet provided by VITROCELL®, which allows for automatically taking into account the 2-fold dilution of the fluorescein concentration of the samples from the insert and QCM.

With the fluorescein-determined DF value, the (upper limit of) the expected transwell insert-delivered solute or particle dose per area (deposition) can be calculated accordingly (Ding et al., 2020):

$$dep = c_{neb} \frac{V_{neb}}{A_{chamber}} DF^{*}1000 \quad (3)$$

dep: solute (or particle) deposition for nebulized solutions (or particle suspensions) (ng/cm^2).

c_{neb}: (known) solute (or particle) concentration in nebulized solution/suspension (μg/mL).

V_{neb}: nebulized volume of solution (or suspension) (0.2 mL).

$A_{chamber}$: total surface area at the bottom of the exposure chamber (141.6 cm^2).

DF: unless stated otherwise the deposition factor of the inserts as derived from eq. 1 is used.

More detailed information and additional remarks can be found in the PATROLS SOP Handbook; https://patrols-h2020.eu/publications/sops/SOP-library-pdfs/3601_2_SOP_PATROLS_Cloud_Aerosolization.pdf?m=1669206589& and the document available for VITROCELL® customers).

2.7. Transmission electron microscopy (TEM)

To investigate and compare the size and morphology of the aerosolized and deposited materials, TEM grids (carbon-coated copper grids; 300 mesh, CF300-Cu, EMS, USA) were placed into a TEM grid holder (VC5036, VITROCELL® Systems GmbH, Germany) and put onto one of the nine inserts of the Cloud device prior to aerosolization. Representative images with a resolution of 2048 × 2048 pixels were obtained via a TEM (FeiTechnai Spirit, Oregon, USA) operating at 120 kV and equipped with a Veleta CCD camera (Olympus, Japan). The images of the samples from AMI, RIVM, BASF, HMGU, and STAMI were recorded at the Adolphe Merkle Institute (AMI, Switzerland). SU (FEI TALOS F200X TEM) and LIST analyzed their samples at their institutes using the same machine operating characteristics.

2.8. Statistical analysis

For statistical analyses, GraphPad Prism 9 software was used. Replicates of the experiments were used for calculating the standard deviation (SD), standard error mean (SEM), coefficient of variation (CV), and mean values. The Wilcoxon test was applied to determining the significance ($p < 0.05$) of differences observed between two groups. For outlier detection, the ROUT method was used.

3. Results

3.1. Material characterization

Data on the physico-chemical characteristics of DQ_{12} and TiO_2 NM-105 are available from the Joint Research Centre (JRC, Italy,) the Fraunhofer IME (Germany), and other published studies (Robock, 1973; Driessen et al., 2015; Bannuscher et al., 2020; Ortelli et al., 2021; Karkossa et al., 2019). Moreover, dynamic light scattering (DLS) analysis was performed on particle suspensions at AMI. The main parameters relevant for this study are presented in Table 1. Most notably, the median hydrodynamic diameter of the particle agglomerates in the stock suspension was found to be below 5 μm, which should be small enough for most of the DQ_{12} and TiO_2 agglomerates to pass through the (> 5 μm) pores of the vibrating mesh nebulizer of the VITROCELL® Cloud12 system.

3.2. Development and optimization of the standard operating procedure (SOP)

During the development of the SOP for the aerosolization experiments with the VITROCELL® Cloud12 system (Fig. 1A), related literature was reviewed, instructions from the manufacturer were considered (VITROCELL® Systems, Waldkirch, Germany), and several procedures were tested to achieve an optimal SOP for performing material aerosolization and deposited dose (deposition) measurements. It had to be considered that some partners had already been trained in using of the device, while others were entirely new to this technology. Therefore, the SOP contains all details needed for beginners, but is also suitable for advanced users.

The SOP for aerosolized substance delivery presented here strongly relies on the methodology described by Ding *et al.* (Ding et al., 2020), but provides more technical details and adopts some modifications. The main one relates to obtaining the QCM measurement at the end of the exposure. In contrast to Ding et al. (Ding et al., 2020), the cover of the exposure chamber (exposure top) was put back on the base module 1 min after it was removed for sample drying (at 480 s of the exposure protocol; Fig. 1B) and QCM data acquisition was stopped 3 min later. This eliminated fluctuations of the QCM signal, possibly due to temperature fluctuation effects induced by the ventilation system of chemical and laminar flow hoods, which the Cloud system is typically placed in for cell culture experiments. Moreover, putting the exposure top back on also minimizes potential bias in the QCM signal due to differences in the temperature of the quartz crystal during zero-setting of the QCM prior to the exposure (with exposure top on) and during dose measurement after the exposure (now also with exposure top on). As an intuitively reasonable but inadequate approach, we also considered not lifting the exposure top for sample drying, but extending the cloud settling and QCM recording ("drying") time from 6 min to 20 min after the start of nebulization - hoping that the prolonged waiting time would allow for complete drying of the QCM even without opening exposure chamber. However, this was not the case. While repeating experiments showed similar temporal profiles of the QCM signal and reasonably reproducible QCM results at the end of the waiting time (tested at AMI

only), the measured mass dose was larger than the theoretically possible maximum dose (assuming a DF of unity (100%) and a solute concentration of 10.58 mg/mL). This is likely due to residual water still residing on the QCM (positive bias) combined with QCM signal bias due to the viscoelastic properties of liquids (negative bias; (Keiji Kanazawa and Gordon, 1985)). Thus, opening the exposure top is crucial for QCM accuracy in the Cloud device and cannot be substituted with prolonged drying under closed exposure top conditions. The PATROLS SOP in its final form was used for the fluorescein assay and material aerosolization (PATROLS SOP Handbook; https://patrols-h2020.eu/publications/sops/SOP-library-pdfs/3601_2_SOP_PATROLS_Cloud_Aerosolization.pdf?m=1669206589&).

3.3. Deposition factor and predicted deposited dose

The deposition factor DF, *i.e.*, the fractional aerosol volume deposited on the bottom of the VITROCELL® Cloud12 exposure chamber, is one of the main performance parameters of the Cloud device. Following the fluorescein assay, 0.2 mL of fluorescein sodium salt-spiked DPBS (fluo-DPBS) was aerosolized, and subsequent, DF was calculated for transwell inserts and QCM using Eqs. 1 and 2, respectively (Table 2). Typically, DF is derived from the deposition onto the transwell inserts. Since here we also derive DF from the deposition in the QCM, the latter is referred to as DF_{QCM}.

The mean, standard deviation (SD), and standard error of the mean (SEM) of the DF obtained for the transwell inserts and the QCM for each of the partner labs can be found in Table 3 and Supplementary Table S1. It is noteworthy, that only the mean DF values based on all eight transwell inserts available in the VITROCELL® Cloud12 device were reported here. Each partner performed $N = 3$–9 independent repeated experiments (see Table S1 for details). From the graphical depiction of the data in Fig. 2A and B, it is evident that the mean DF in the insert varied between 0.392 and 0.865 among the seven partner labs, with a mean and coefficient of variation (CV) of 0.635 and 28%, respectively. Similarly, the mean DF_{QCM} values of the QCM measured by the partners varied between 0.320 and 0.888, yielding a mean value of 0.597 and a CV of 33%, respectively (see Table S1). There was no statistically significant difference between the mean DF values of 0.635 and 0.597 obtained for the inserts and the QCM, respectively, and the CV was close to 30% for both inserts and QCMs. This indicates that on average (over seven different Cloud systems) the dose of fluorescein (and its variability) which reached the transwell inserts was identical to that indicated by the QCM, which is a prerequisite of the QCM serving as dose monitor for cell−/insert-delivered particle dose.

For the QCM itself, one can compare the fluorescence-derived fluosalt (here: fluo-DPBS) dose with the QCM-recorded signal. It is evident from Fig. 2C that despite significant variability of deposition observed by the various partners (between 5000 and 13,500 ng/cm^2) there was agreement between fluorescence- and QCM-monitored deposition within statistical uncertainty, except for STAMI, who observed a 2.0-fold higher dose from fluorescence analysis. However, for actual exposure experiments it is more important to compare the QCM signal with the fluorescence-spiked DPBS (fluo-DPBS) dose in the inserts, since the QCM signal is supposed to represent the transwell insert-delivered dose. Fig. 2D shows that SU, BASF and STAMI observed statically significant differences between both values. To interpret this result, it is instructive to consider the ratio of these deposition values for each partner, where here the error bars represent SD to give an impression of the variability between repeat experiments (Fig. 2E). Ideally, the transwell insert/QCM deposition factor or dose ratio is unity, *i.e.,* no dose conversion factor has to be applied to the QCM values. The observed dose ratio of STAMI (1.61) was significantly different from unity. All other dose ratios were between 0.90 and 1.32 without being significantly different from unity, except for BASF (1.14), which had the lowest SD (±0.05) compared to all other partners, indicating that their experiments were more reproducible. This explains why BASF did not report a statistically significant QCM conversion factor. The implications of this will be addressed in the discussion section.

Table 3
Overview of inter-laboratory comparison of the results from the fluorescein assay (DF on transwell inserts and on QCM) for the seven partner laboratories. Moreover, the DF_{QCM} value was employed to predict the fluo-DPBS deposition on the QCM (using Eq. 3) and this value was compared to the actually recorded QCM signal.

	DF (in inserts)	DF_{QCM}	Fluo-DPBS deposition on QCM calculated from DF_{QCM} (ng/cm^2)	Fluo-DPBS deposition on QCM according to QCM signal (ng/cm^2)
Minimum	0.392	0.320	4773	5027
Maximum	0.865	0.888	13,258	13,590
Range	0.473	0.568	8485	8563
Mean	0.635	0.597	8969	8806
SD	0.175	0.197	2983	2881
SEM	0.066	0.075	1127	1089
Coefficient of variation (CV)	28%	33%	33%	33%
p-Value	$p = 0.5781$ n.s.		$p = 0.4688$ n.s.	

3.4. Deposition of DQ_{12} and of TiO_2 NM-105

Aerosolization of increasing concentrations of DQ_{12} and TiO_2 NM-105 suspensions (0, 125, 250 and 500 μg/mL), which was tested at AMI prior to conducting the inter-laboratory experiment, resulted in a linear increase of the QCM signal (Fig. 3A and B; $R^2 > 0.95$). For the vehicle itself without any particles, the QCM reported a dose of 45 ± 21 ng/cm^2 and 50 ± 21 ng/cm^2 for the DQ_{12} and TiO_2 experiments (Fig. 3A and B), respectively. The slopes of the blank-corrected deposition-concentration curves of the QCM (forced through the origin) were 0.934 and 0.707 ng/cm^2/(μg/mL) for DQ_{12} and TiO_2, respectively (Fig. 3A and B).

Table 2
Deposition of fluorescein-spiked DPBS - "fluo-DPBS" - in the inserts and on the QCM and in the transwell inserts, where the former represents the QCM signal and the latter was determined from DF of the inserts (fluorescein assay) and Eq. 3 (10.58 mg/mL fluo-DPBS concentration; 0.2 mL aerosolized liquid).

Participant	Fluo-DPBSdeposition (ng/cm^2)							
	on QCM (QCM signal)				in inserts			
	Mean	SD	SEM	N	Mean	SD	SEM	N
AMI	8563	1297	530	6	9624	1235	437	8
RIVM	13,590	1432	477	9	12,926	793	162	24
SU	8940	618	252	6	7606	1867	660	8
BASF	11,282	332	136	6	12,700	419	148	8
LIST	5027	818	334	6	5858	430	152	8
HMGU	7734	1765	1019	3	9654	480	170	8
STAMI	6509	759	438	3	8025	510	180	8

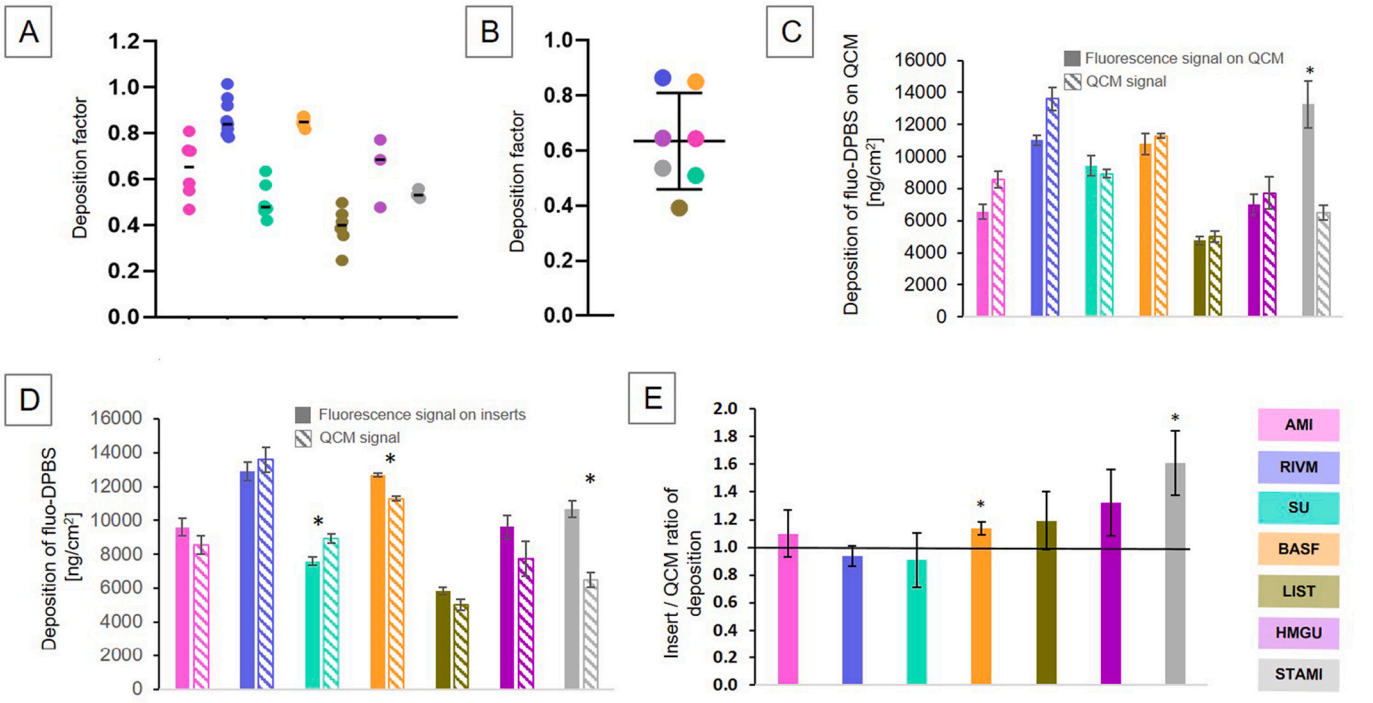

Fig. 2. Inter-laboratory comparison of the fluo-DPBS deposition in the VITROCELL® Cloud 12. A: Deposition factor (DF) measured by fluorescence on the transwell inserts (mean of 8 inserts) at the seven partner laboratories, which performed $N = 3–9$ independent experiments, B: Inter-laboratory comparison of mean DF values based on data from panel A (mean and 95% CI), C: Deposited fluo-DPBS (salt) dose (mean ± SEM, N = 3–9) on the QCM obtained from the fluorescence signal (from DF_{QCM} and Eq. 3) as compared to the QCM signal. Only STAMI reports a statistically significant difference between fluorescence- and QCM-derived deposition. D: Salt deposition in inserts (mean ± SEM for N = 3–9: calculated from DF (insert) and Eq. 3) as compared to the QCM signal. SU, BASF, and STAMI reported a statistically significant difference between both values. E: The ratio (mean ± SD) of salt deposition in the inserts (fluorescence) and on the QCM (QCM signal) agreed within statistical uncertainties except for BASF and STAMI. Partner institutes are represented in different color codes. *$p < 0.05$.

The observed DQ_{12} and TiO_2 deposition curves are consistent with the doses predicted from DF_{QCM} and the known particle concentration of the aerosolized suspensions (grey shaded area) (Fig. 3C).

For the interlaboratory comparison study, only the highest dose was pursued. The deposition of aerosolized 500 μg/mL DQ_{12} and TiO_2 NM-105 suspensions (without blank correction) observed by all partner laboratories are listed in SI Tables 3 and 4, respectively, and depicted in Fig. 3D. While most of the particle deposition was between 350 and 525 ng/cm^2, six data points (mostly TiO_2) were below this range (minimum: 174 ng/cm^2). In general, DQ_{12} deposition showed larger values and less variability (mean = 449 ng/cm^2; CV = 27%) than TiO_2 deposition (mean = 326 ng/cm^2; CV = 37%). Looking at each partner laboratory separately, three out of seven partners found the same deposition value for both DQ_{12} and TiO_2 (* $p < 0.05$). Moreover, LIST and HMGU reported elevated blank values of 153 ng/cm^2 and 193 ng/cm^2, respectively, as compared to the other laboratories (<87 ng/cm^2). However, all particle deposition values were above the respective blank values ($p < 0.05$) (Fig. 3D). For a more in-depth analysis of the results, the particle deposition values were blank-corrected to obtain the actual particle-induced dose reported by the QCM (Fig. 3E). It is important to note that for individual exposure runs the measured blank values can be below zero due to instrument noise near the detection limit of the QCM. Thus, negative values have to be also included in the calculation of the mean and SD of the blank deposition. These values are reported in SI Tables 3 and 4 and depicted in Fig. 3E and the statistical analysis of the mean values from all partner labs is presented in Table 4. Subtraction of the blank values reduced the mean deposition of DQ_{12} and TiO_2 particles from 449 ng/cm^2 to 367 ng/cm^2 (CV = 32%) and from 326 ng/cm^2 to 244 ng/cm^2 (CV = 48%), respectively. Again, these values are not significantly different due to the relatively high CV. The notable increase of CV (DQ_{12}: from 27% to 32%; TiO_2 NM-105: from 37% to 48%) can at least partially be attributed to the statistical uncertainty of the subtracted blank values (laws of error propagation). It is evident from Fig. 3E, that only AMI, SU, LIST (DQ_{12} only) and STAMI (DQ_{12} only) observed an agreement between predicted and measured particle doses ($p < 0.05$), for all other cases the measured particle doses were lower than predicted. The observed large CV is at least partially due to the different DF of the Cloud 12 devices. This effect can be accounted for by normalizing the (blank-corrected) particle deposition to the device-specific *predicted* deposition (henceforth referred to as *normalized dose*) leveraging eq. 3 and the device-specific DF values (Table 5). The *normalized dose* of 0.91 (45%) for DQ_{12} indicates that the measured DQ_{12} doses agree with the predicted dose levels (9% lower measured than the predicted dose). On the other hand, the observed TiO_2 NM-105 doses are 1.9-fold lower than predicted (mean ratio of 0.54 (41%)). For reasons discussed below, this did even increase CV and, therefore, the differences in mean normalized doses are still not statistically significant.

3.5. TEM images

It was important to also visually show that the aerosolized particles deposit on the TEM grids placed on the permeable inserts. DQ_{12} and TiO_2 NM-105 aerosolized onto TEM grids were analysed by TEM imaging (Figs. 4-6). The initial experiments conducted at AMI with increasing stock concentrations revealed increasing particle numbers on the TEM grids. For the highest stock concentration, *i.e.,* 500 μg/mL, agglomerates became visible for both materials (Fig. 4).

The other partner laboratories only aerosolized the highest stock concentration, *i.e.,* 500 μg/mL, for both particle types. Similar TEM images were obtained for both TiO_2 NM-105 and DQ_{12}. The TEM images of the aerosolized DQ_{12} particles displayed both small and large DQ_{12} particles, with wide variations in size distribution observed for the various participants (Fig. 5). Also the TEM images of TiO_2 NM-105 samples from each laboratory showed that particle agglomerates were

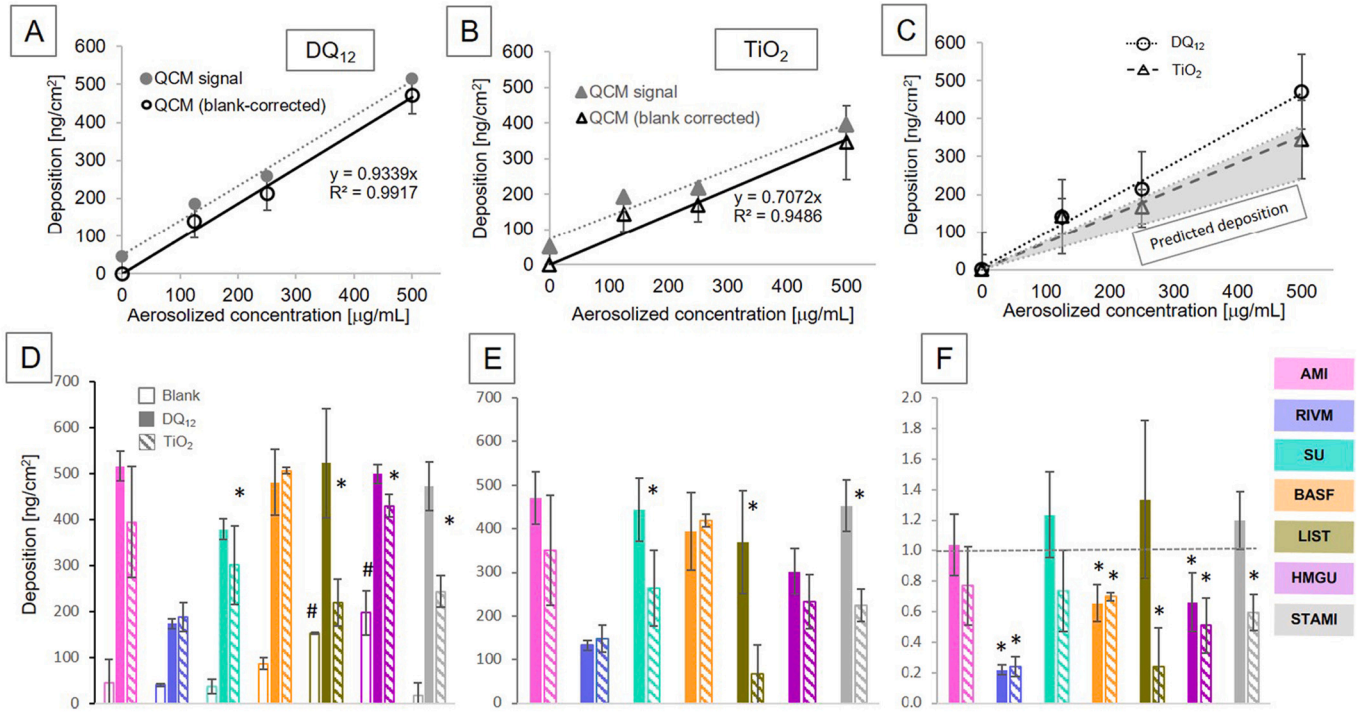

Fig. 3. Inter-laboratory comparison of NM deposition in VITROCELL® Cloud12. A: Dose range experiment performed at AMI for 0, 125, 250 and 500 µg/mL DQ_{12} suspensions ($N = 6$) demonstrated good linearity of the QCM signal ($R^2 > 0.99$) (mean ± 95% CI). For a more accurate particle dose, the respective blank values were subtracted. B: Same as panel A, but for TiO_2. C: The blank-corrected deposition curves for DQ_{12} and TiO_2 are consistent with the concentration-dose curves predicted from DF (eq. 3; grey shaded area (mean ± SD). D: Deposition after nebulization of a 500 µg/mL DQ_{12} and TiO_2 NM-105 suspension and of the vehicle (blank) observed by the partner laboratories. Four of the seven partner labs show lower deposition values for TiO_2 than for DQ_{12} (*$p < 0.05$). LIST and HMGU reported elevated blank values as compared to the others ($^{\#}p < 0.05$) (mean ± SD). E: For the more relevant blank-corrected deposition values only three partners (SU, LIST, STAMI) reported lower deposition values for TiO_2 than for DQ_{12}. For reference, the DF-predicted dose values for each device are also depicted (mean ± SD; * $p <$ 0.05). F: Same as E, but for each device the DQ_{12} and TiO_2 deposition are normalized to their predicted dose value (normalized dose). This illustrates that 8 out of the 14 measured particle doses are lower than their predicted value (mean ± 95% CI; *$p < 0.05$). Partner institutes are represented in different color codes.

Table 4
Overview of inter-laboratory comparison results of DQ_{12} and TiO_2 NM-105 particle deposition measured by the QCM. Blank-corrected values are indicated in parentheses.

	Blank	DQ_{12} 500 µg/mL	TiO_2 NM-105 500 µg/mL
Number of values (Participants)	7	7	7
Minimum (ng/cm^2)	19.0	174 (133)	189 (67.0)
Maximum (ng/cm^2)	197.3	523 (471)	506 (419)
Range (ng/cm^2)	178.3	349 (338)	317 (352)
Mean	82.8	449 (367)	326 (244)
SD	67.5	1223 (118)	119 (118)
SEM	25.5	46.5 (44.7)	45.0 (44.5)
Coefficient of variation (CV)	81.5%	27.4% (32.3%)	36.5% (48.4%)

present, again with a wide variations in size distributions (Fig. 6).

4. Discussion

Albeit the physiological advantages of ALI lung cell culture models for toxicological assessment of aerosolized materials such as micron-sized and nano-particles have been widely acknowledged (Paur et al., 2011; Hiemstra et al., 2018; Lacroix et al., 2018; Ehrmann et al., 2020), wide-spread use of such lung models has been hampered in part due to absence of aerosol-cell exposure systems which are easy-to-use, dose-controlled and suitable for delivering sufficiently high but also relevant doses in a relatively short time (< 1 h). In the past few years the commercially available VITROCELL® Cloud technology for 6- and 12-well transwell inserts has become increasingly more widely used. Inter-laboratory comparison studies are now an important next step towards harmonized and standardized operation as prerequisite for potential regulator acceptance of these devices for *in vitro* hazard testing.

The selected seven laboratories covered the levels of expertise ranging from complete beginners to the inventor of the ALICE-/VITROCELL®-Cloud technology (HMGU). Moreover, the VITROCELL® Cloud12 comparison was performed with soluble fluorescein-spiked salt (fluo-DPBS) and two types of non-soluble (poorly soluble) particles, *i.e.*, DQ_{12} and TiO_2 NM-105. The fluo-DPBS allowed for assessment of device-specific performance differences and validation of the QCM for transwell insert-deposited dose measurement. The chosen particles elucidated potential additional complications due to the use of particles rather than molecular substances, *e.g.* water-soluble chemicals. For the particle study a dose relatively close to the detection limit of the QCM-dosimetry method was selected (ca. 250–500 ng/cm^2, depending on device and particle type), which makes the study applicable to most of the cases where reliable values for dose-response curves can be obtained with the Cloud 12 system.

4.1. Standard operating procedure (SOP) for the aerosolization of materials using the VITROCELL® Cloud12 system

The basis for this inter-laboratory comparison study was a detailed SOP for the VITROCELL® Cloud12 system, which was developed within the H2020-funded PATROLS project (Physiologically Anchored Tools for Realistic nanOmateriaL hazard aSsessment; PATROLS SOP Handbook, https://patrols-h2020.eu/publications/sops/SOP-library-pdfs/3601_2_SOP_PATROLS_Cloud_Aerosolization.pdf?m=1669206589&).

Table 5
Overview of DF-predicted (upper limit), QCM-measured (blank-corrected) and normalized delivered particle dose for each partner laboratory (DF is unitless, doses in ng/cm^2 and CV in %). The (upper limit) of the deposited particle dose was predicted from Eq. 3 using the partner-specific DF values (in inserts; Table S1), the known concentration of the particle suspension (500 µg/mL), and the nebulized volume of particle suspension (0.2 mL). The normalized dose refers to the ratio of measured and predicted dose, which relates the QCM-measured particle dose to the corresponding dose one would expect to observe for nebulization of the same saline concentration (500 µg/mL).

	Lab 1 (AMI)	Lab 2 (RIVM)	Lab 3 (SU)	Lab 4 (BASF)	Lab 5 (LIST)	Lab 6 (HMGU)	Lab 7 (STAMI)
DF (CV)	0.644 (20.0)	0.865 (9.4)	0.509 (15.7)	0.850 (2.5)	0.392 (22.0)	0.646 (23.4)	0.537 (3.8)
Predicted Deposited Dose (CV)	455 (20.0)	611 (9.4)	359 (15.7)	600 (2.5)	277 (22.0)	456 (23.4)	379 (3.8)
Measured Deposited Dose of DQ_{12} (CV)	471 (12.8)	133 (8.6)	444 (16.4)	394 (18.3)	370 (39.7)	302 (17.3)	453 (13.1)
Measured Deposited Dose of TiO_2 NM-105 (CV)	350 (36.6)	148 (21.1)	264 (32.8)	419 (3.5)	67.0[a] (101)	232 (30.0)	225 (17.2)
Normalized DQ_{12} Dose (2 *SEM)	1.04 (0.20)	0.21[b] (0.03)	1.23 (0.28)	0.67[b] (0.12)	1.34 (0.52)	0.66[b] (0.19)	1.19 (0.19)
Normalized TiO_2 NM-105 Dose (2*SEM)	0.77 (0.26)	0.24[b] (0.06)	0.74 (0.27)	0.70[b] (0.03)	0.24[a,b] (0.25)	0.51[b] (0.18)	0.59[b] (0.12)

[a] This value is not significantly different from zero ($p < 0.05$). This is possibly due to problems with preparing a stable particle suspension.
[b] Significantly lower than unity, *i.e.,* the measured dose is lower than the predicted dose ($p < 0.05$).

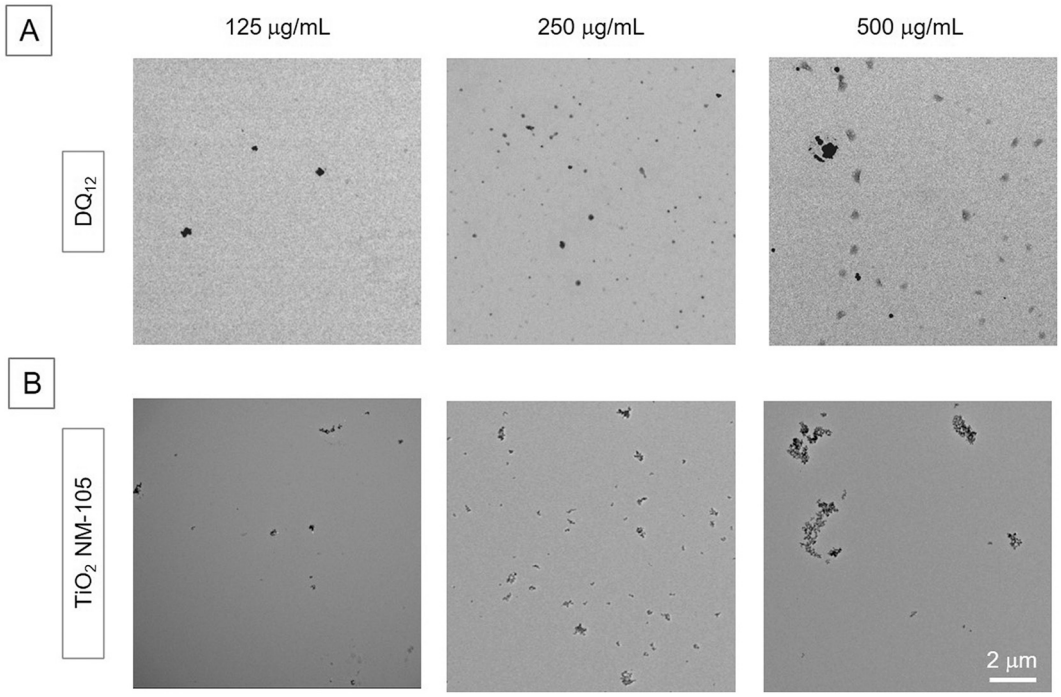

Fig. 4. TEM images of aerosolized DQ_{12} and TiO_2 NM-105 in the VITROCELL® Cloud12 system in partner laboratory 1 (AMI). A: Deposition of DQ_{12} and B: of TiO_2 NM-105 after aerosolization of different stock concentrations. Scale bar = 2 µm for all images.

The SOP was written according to GIVIMP guidelines (OECD, 2018) for the aerosolization of DQ_{12} and TiO_2 NM-105 as representatives of widely used micron- and nano-sized materials. Therein, we describe in detail the setup of the system and a general procedure to optimally perform aerosolization of materials, as well as how to determine the transwell insert-deposited dose. In addition, we explain how to determine threshold values for blank exposures as a measure of quality control for clean operating conditions and provide recommendations for cleaning the nebulizer, the exposure system and the QCM to ensure proper working conditions (see also this YouTube video about VITROCELL® Microbalance Cleaning Procedures: https://www.youtube.com/watch?v=HE0AGAvabck, accessed 23 July 2022). This threshold value was set to 250 ng/cm^2, which takes into account i) that the required addition of 90 µg/ml NaCl into the vehicle (water) results in a blank (NaCl) dose of up to 128 ng/cm^2 (calculated from eq. 3 assuming DF = 1), ii) the possible presence of other impurities in the vehicle can result in a blank value even larger than 128 ng/cm^2 (if impurities in addition to the NaCl spiking are contained in the water) and iii) the previously reported lower limit of detection for QCM-based dosimetry in the VITROCELL® Cloud 12 system of 98 ng/cm^2 (=170/SQRT(N) ng/cm^2 with $N = 3$) (Ding et al., 2020).

For the QCM, we slightly modified the procedure described by Ding *et al.* (Ding et al., 2020), *e.g.* the removed lid of the exposure chamber is placed back after complete drying of the sample. This provides identical thermal conditions as present during setting of the zero point of the QCM (just prior to start of aerosolization) resulting in further reduction of QCM fluctuations due to matching the temperature conditions of the QCM prior and after exposure. This step can often be skipped, provided the user has experimentally confirmed that the QCM signal does not change by more than a few percent if the exposure top is removed and placed back again.

In this inter-laboratory comparison study, we have noticed that some partners experienced problems and needed assistance, despite the detailed SOP. One of the main problems was that the quartz crystals of the QCM were used too many times without in-depth cleaning. VITROCELL® Systems recommends always using a cleaned crystal for a new aerosolization.

Aerosolization of 200 µL of water spiked with 0.0009% (=90 µg/mL)

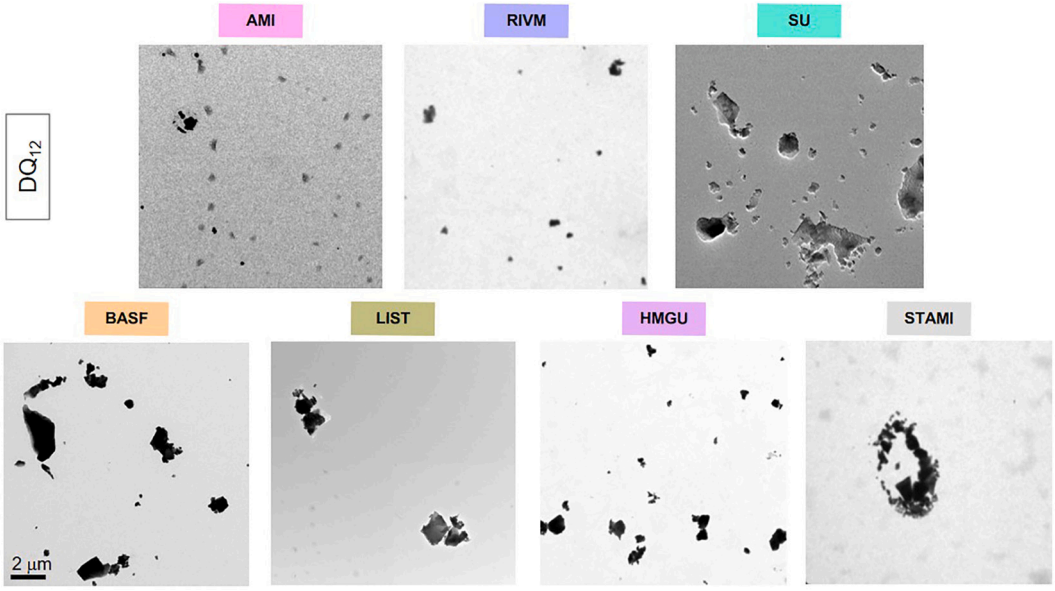

Fig. 5. TEM images of deposited DQ_{12} in the VITROCELL® Cloud12 system for inter-laboratory comparison. Scale bar = 2 µm for all images.

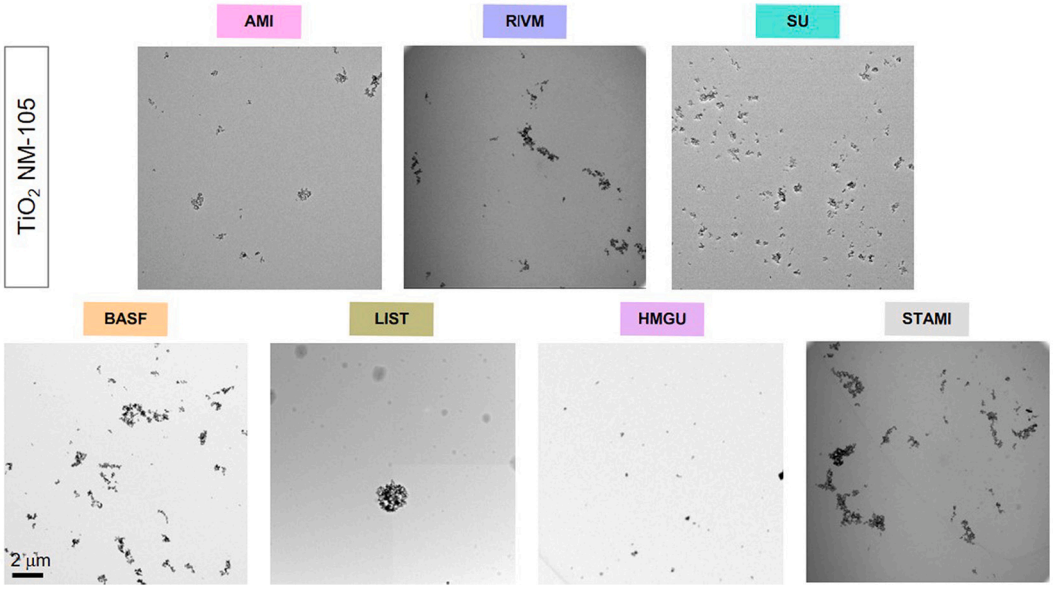

Fig. 6. TEM images of deposited TiO_2 NM-105 in the VITROCELL® Cloud12 system for inter-laboratory comparison. Scale bar = 2 µm for all images.

NaCl as used here is expected to result in 51 to 128 ng/cm^2 deposited (NaCl) dose (blank control) as calculated from eq. 3 with DF values typically ranging from 0.39 to 1.0 in the present study and as described (Lenz et al., 2014; Ding et al., 2020; Röhm et al., 2017). It is important to note that these values are near the detection limit of the QCM, which was reported as 170 ng/cm^2/SQRT(N) (Ding et al., 2020). This implies that the detection limit for the mean blank value derived from $N = 3$ and $N = 6$ repeat measurements corresponds to 98 ng/cm^2 and 69 ng/cm^2 (SEM), respectively. Please note, that also negative QCM values need to be included in this average as the instrument noise can result in negative values. In many cases the NaCl-spiking of the aerosolized liquid results in a deposited dose below the detection limit of the QCM. In this case, it is recommended to either increase the number of repeat measurements (preferred option) or to calculate the predicted blank value from eq. 3 (assuming 90 µg/mL NaCl accounts for the blank signal). If statistically significant higher blank values than predicted from eq. 3 are observed, there are either additional impurities in the nebulized liquid or it indicates a problem with the QCM which might indicate the need for proper cleaning or even replacement of the quartz crystal. If the latter was required, visual inspection often showed scratches on the crystal. Another technical problem we occasionally observed was clogging of the approximately 5 µm pores of the vibrating mesh nebulizers with poorly soluble DQ_{12} or TiO_2 particles. This can substantially reduce the output rate of the nebulizer for isotonic saline (0.2–0.8 mL/min depending on the nebulizer) by more than 10% of its initial value, and it can be resolved by performing the extended nebulizer cleaning procedure as described in the SOP. The acceptable time range for nebulizing 200 µL of water/suspension is between 15 and 60 s (0.2–0.8 ml/min) and all partners only considered experiments where the nebulization time was below 60 s. Prolonged aerosolization time can be a sign of a blocked nebulizer, therefore it needs to be cleaned thoroughly or replaced. Partners also experienced disruption of the QCM signal (a sudden signal jump to extremely low negative mass values) while the quartz crystal was wet, which often could be resolved by replacing the connecting

cables or technical assistance from VITROCELL® Systems. In some instances, this issue could not be resolved, but the QCM typically returned to regular operation after the drying step in the exposure protocol. Thus, the QCM resumed regular operation during the last 3 min of the exposure experiment, which allowed for robust dose measurement. Overall, most of the technical problems with the QCM can be resolved by an operator with QCM experience, and all laboratories were ultimately able to report reproducible and robust QCM data. To conclude, for new users of this SOP, webinars and on-site training is recommended. It is noteworthy, that VITROCELL® Systems introduced a new type of QCM (sQCM 12) shortly after this study allowing for more stable QCM operation.

4.2. Inter-laboratory comparison of fluorescein and particle aerosolization

The inter-laboratory comparison of the VITROCELL® Cloud12 system is performed in two steps: First aerosolization of fluorescein-spiked saline and associated salt deposition is leveraged to determine device-specific differences in aerosol deposition and verify the QCM for measurement of the transwell insert-deposited particle dose. Subsequently, potential complications associated with aerosolization of particle suspensions are investigated while accounting for device-specific non-particle related performance differences (from fluorescein-spiked saline data).

4.2.1. Fluorescein assay

Device-specific performance differences can be investigated by aerosolization of fluorescein-spiked saline since this water-soluble molecular substance experiences (almost) no loss in the vibrating mesh nebulizer. This was verified experimentally by measuring the aerosolized volume of fluo-DPBS by gravimetric analysis of the nebulizer (before and after aerosolization) and subsequent quantitative spectrofluorometric analysis of aliquots of the aerosolized liquid (data not shown). This also revealed that typically 1% to 3% of the invested liquid (here 0.2 mL) is not converted into aerosols (data not shown). Thus, the expected maximum DF is between 0.97 and 0.99 (here assumed to be unity). The observed DF range between 0.39 and 0.87 extends the previously reported DF range (0.5–1.0; (Lenz et al., 2014; Ding et al., 2020; Röhm et al., 2017)) to somewhat lower values. This indicates that depending on the VITROCELL® Cloud12 exposure system and/or operator-specific handling, between 0% and 61% of the invested amount of substance does not reach the bottom of the exposure chamber. Once the device-specific DF is known (fluorescein assay), eq. 3 can be used to predict the (maximum possible) transwell insert-delivered dose for given experimental conditions (volume and solute/particle concentration of nebulizer liquid). This prediction provides a maximum dose since it assumes no aerosol loss or retention of the solute/particles in the nebulizer, which may not always be the case (see below). It is also noteworthy that the repeatability of dosing, *i.e.,* the variability of dose delivered to all eight inserts of the VITROCELL® Cloud12 system, is given by the CV of the DF, which varies between 2.5% and 23% about the mean value of 13.8% (Table 5). The mean value is consistent with the previously reported 9.3% reproducibility of repeated dosing for a prototype version of the VITROCELL® Cloud 6 system (Lenz et al., 2014). The reason for this 9-fold span of dose reproducibility (2.5% to 23%) is not known, but this will not have a substantial effect on the accuracy of reported dose-response curves, since the exact cell-delivered dose for each exposure run can be measured with the VITROCELL® Cloud12 -integrated QCM.

The reliability of the QCM for accurate dosimetry was demonstrated by comparing the transwell insert-delivered dose or DF value of fluo-DPBS and the corresponding QCM signal. No statistically significant difference between the mean DF values of 0.635 and 0.597 for the transwell inserts and the QCM, respectively, was observed with an almost identical CV of close to 30%. This is a first indication that the QCM accurately measures the dose delivered to the transwell inserts. Looking at each of the seven devices separately, we found that out of the seven devices under investigation only two (BASF and STAMI) displayed statistically significant differences between QCM and insert dose with an associated QCM dose conversion factor of 1.14 (±0.05; 95% confidence interval (CI)) and 1.61 (±0.27; 95% CI), respectively (Fig. 2E). Since dose changes of less than 20% often do not correspond to statistically significant changes in cell-based toxicological assays, one might also discard QCM conversion factors of less than 20% (*i.e.,* between 0.8 and 1.2), even though they may appear as statistically significant (as for the BASF device). However, for more dose-sensitive toxicological assay, even statistically significant QCM conversion factors between 0.8 and 1.2 should be accounted for by dividing the measured QCM dose by the QCM conversion factor.

One of the possible reasons for differences between insert- and QCM-deposited doses could be a not perfectly homogeneous deposition profile of the aerosol in the exposure chamber. This can be assessed by considering the insert-to-insert dose variability of the VITROCELL® Cloud12 system. For fluoro-DPBS, there was less than 9.8% dose variability for each run (relative to the mean dose per insert averaged over all eight inserts) with an instrument average of 8.1% (SD: 2.3%), which is consistent with the previously reported range of <8.3% for a VITROCELL® Cloud12 system (Röhm et al., 2017). Two partners observed a significantly larger insert-specific dose variability of 21.3% (AMI) and 42.6% (SU). The exact reason for these high values could not be identified. However, it may be due to misalignment of the nebulizer, inadvertent contact between the distilled water in the wells and the transwell insert, or even poor quality of the inserts (previously, leaky inserts have occasionally been delivered to some of the partner labs). The QCM is positioned in one of the corner wells of the exposure chamber, which have a higher propensity of deviating from the mean dose received in the other (more centrally located) wells (data not shown). For the seven VITROCELL® Cloud12 devices investigated here, the systematic bias in any of the three other corner wells was less than 20%. Hence, the 1.61-fold STAMI QCM conversion factor is not likely due to limited non-uniformity of aerosol deposition in the Cloud12. For reasons elucidated below, the relatively high 1.61-fold QCM conversion factor for the STAMI device was deemed false - it was not included in the following analysis of the particle-related dosimetry analysis. This implies that the QCM12 provides sufficiently accurate transwell insert-deposited dose values for VITROCELL® Cloud12 devices without applying any conversion factor. This is consistent with the results reported by Ding et al. (2020). Thus, no QCM conversion factor was applied to the particle dosimetry data.

4.2.2. Particle deposition

One of the main objectives of the present study was an inter-laboratory assessment of the VITROCELL® Cloud12 system for efficient, dose-controlled and reliable delivery of two types of particles to transwell inserts. The first critical step was to prepare comparable dispersions of the particles. Protocols for reliable and reproducible preparation for particle dispersions were used, including guidance on sonification, and if necessary adjusted as indicated. Agglomerates of different sizes were observed in TEM images, which could be due to dispersion variety, but we did not investigate this further as similar size differences were also observed for different exposure runs performed by the same laboratory.

Adhering to the SOP all partner laboratories performed blank exposures prior to particle exposures to allow for accurate blank correction and to verify clean and proper working conditions of the VITROCELL® Cloud12, as indicated by blank values below the threshold of 250 ng/cm^2. The absence of particles was also confirmed for selected blank exposures using TEM images. The selection of 500 μg/mL particle concentration in the aerosolized suspensions was based on the intent to perform the comparison study in the most challenging, *i.e.,* lowest possible dose range, *i.e.*, close to 250 ng/cm^2. Considering that the

lowest reported DF value is 0.39, nebulization of 0.2 mL of a 500 μg/mL particle suspension would result in a maximum dose of 277 ng/cm^2, which was considered the lowest possible and thus most challenging condition suitable for this inter-laboratory comparison study. Notably, this dose range is close to the cytotoxic dose of 390 ng/cm^2 observed for high-hazard zinc oxide (ZnO) nanoparticles deposited on A549 lung epithelial cells (Ding et al., 2020). Since (nano)particles with higher hazard potential (may) induce toxicological effects at lower doses, the QCM detection limit only becomes a problem for extremely high hazard materials.

As prerequisite for a reliable inter-laboratory comparison study, the linear relationship between particle concentration and particle deposition was experimentally confirmed by one of the laboratories (AMI) using TEM images and QCM-based particle concentration-dose measurements between 0 and 500 μg/mL for DQ_{12} and TiO_2 NM-105. The QCM data emphasized the relevance of blank correction (mainly due to NaCl-spiking of the vehicle – here water) for accurate particle dosimetry and the reliability of DF-based prediction of the (upper limit) of the device-specific deposited dose. These aspects are essential for interpreting the observed differences in DQ_{12} and TiO_2 NM-105 deposition, which can be due to either particle-specific effects (*e.g.*, particle retention in the nebulizer) or device-specific deposition efficiency characterized as DF or both. As a caveat, we add that only blank-corrected deposition values should be considered for dose-response curves and interlaboratory comparison studies. For experimental planning, it may be useful to consider that an estimated blank correction can be calculated from eq. 3. For DF values ranging between 0.4 and 1.0 (see Fig. 2b and (Lenz et al., 2014; Abubakar et al., 2015)), a lower limit of the impurity concentration of 90 μg/mL NaCl (NaCl-spiking of the NM suspension for reliable operation of the nebulization) eq. 3 yields blank values between 51 and 128 ng/cm^2. It is important to note that blank corrections larger than 128 ng/cm^2 are also possible, since the vehicle may contain additional impurities due to e.g. imperfect water purity or residues in the nebulizer. Thus, actual measurement of the blank value (equivalent to sham control for biological endpoints) and its subtraction from the measured NM dose is required for accurate dosimetry, especially in the low dose range of <500 μg/mL NM suspension, where the 90 μg/mL NaCl impurities itself accounts for a 18% positive bias in measured NM dose, if the blank correction is not applied.

Out of the seven laboratories, four partners did not report statistically significant differences between DQ_{12} and TiO_2 NM-105 deposition and three partners found statistically significantly lower TiO_2 NM-105 deposition (SU, LIST, STAMI). This indicates that the deposited dose of the VITROCELL® Cloud12 can depend on the type of material aerosolized. However, it is not clear from this data if the Cloud systems behaved differently for particles than for saline. This can be investigated by considering normalized QCM values, *i.e.,* the measured particle deposition is normalized to the dose predicted for nebulization of 500 μg/mL saline. The normalized dose of TiO_2 NM-105 (0.54) is significantly lower than that of DQ_{12} (0.91), but the normalized dose of DQ_{12} is not different from that of saline (1.0, per definition). This can be explained by the well-known tendency of TiO_2 NM-105 particles to form agglomerates in aqueous suspension without stabilization by proteins (*e.g.*, serum proteins). As these agglomerates may not be able to pass through the mesh of the nebulizer, this may result in a lower deposition of TiO_2 NM-105. The former may partially or entirely block the nebulizer, which was observed more frequently for TiO_2 NM-105 and repeated thorough cleaning became imperative to ensure proper operation of the VITROCELL® Cloud12 system. Nebulization of less concentrated particle suspensions combined with repeated exposures may alleviate clogging of the nebulizer. Moreover, for quality control it is important to repeatedly measure the duration of the aerosolization process (*i.e.,* the output rate of the nebulizer) as a change in aerosolization time can indicate (partial) clogging or degradation of the nebulizer. Albeit VITROCELL® Cloud12 performance does not strongly depend on nebulizer output rate, replacement of the nebulizer has to be considered as the ultima ratio if irreversible changes in nebulization time of *e.g.* larger than 20% occur. All of the aspects mentioned above and some additional details are also integrated in the SOP (see sec. 6.2 and 6.3)

The potential for reduced aerosolization of materials such as nanoparticles as compared to molecular substances (*e.g.* saline) indicates that the saline-based DF provides an upper limit of the DF values observed for nanoparticles. The actual DF of nanoparticles depends on numerous parameters, including size and stability of the nanoparticles in suspension, adsorption of nanoparticles to the walls of the reservoir volume of the nebulizer, and clogging of the nebulizer membrane. This highlights the relevance of considering the behavior of nanoparticles during the aerosolization process. However, it is important to note that despite potentially reduced deposition of nanoparticles, the QCM ensures accurate dose information independent of the efficiency of the aerosolization process.

For DQ_{12}, the lowest DF value of 0.22 measured by RIVM was identified as an outlier (ROUT method). Removing this value increases the mean normalized dose of DQ_{12} from 0.91 to 1.0 and reduces CV from 45% to 29%, corresponding to the CV value for saline. This indicates that the VITROCELL® Cloud12 system aerosolizes DQ_{12} as well as saline. Since the DLS size distribution measured by RIVM did not show any evidence of instability of the aerosolized DQ_{12} suspension, it is conceivable that there was a technical problem with the QCM. This is corroborated by the fact that the normalized TiO_2 NM-105 dose for RIVM was also extremely low (0.24), yet not an outlier since LIST reported the same normalized TiO_2 NM-105 value. Thus, the mean and CV of the normalized TiO_2 NM-105 dose remains at 0.54 and 41%, respectively, which is consistent with agglomerate formation and associated lower and more variable aerosolization and deposition.

The excellent aerosolization properties of DQ_{12} allow for a reassessment of the previously derived QCM conversion factor of 1.61 for the STAMI device (Fig. 2E), which has not been included in any of the values shown above. If this conversion would be applied, the normalized DQ_{12} dose would increase to 1.9, rendering it not only an outlier within the DQ_{12} data, it would also imply than more DQ_{12} mass would have reached the bottom of the exposure chamber than would have been put into the nebulizer. Moreover, the STAMI QCM data for both DQ_{12} and TiO_2 are consistent with those from the other labs. Taken together, this indicates that the 1.61-fold QCM conversion factor derived from the fluorescein assay has to be considered false. The reason for this is unknown, but it may have been associated with poor QCM performance during the fluo-DPBS experiments (not during the particle experiments).

5. Conclusions

Inter-laboratory studies are essential for implementation of ALI lung cell cultures as a more predictive approach for *in vitro* hazard assessment of aerosolized materials as well as for regulatory acceptance. The aim herein was to assess the performance of the commercially available VITROCELL® Cloud12 systems operated by seven different laboratories using a common SOP developed within the Horizon 2020 funded PATROLS project. This study focused on QCM-based measurement of the cell-delivered dose for DQ_{12} and TiO_2 NM-105 particles.

The seven partners represented a wide range of expertise in VITROCELL® Cloud12 operation, from absolute beginners to most experienced users. The investigated particle dose of 250–500 ng/cm^2 (depending on device and particle type) was selected to work under worst-case conditions, *i.e.,* near the lower limit of the detectable dose (<170 ng/cm^2 for a single exposure; <170/sqrt(N) ng/cm^2 for N repeat exposures (Ding et al., 2020). The device-specific deposition factor (DF) for fluorescein-spiked saline is a valuable tool for predicting the upper limit of the expected transwell insert-delivered dose of any investigated material aerosolized with the VITROCELL® Cloud technology. The exact reasons for the observed ca. 2-fold variability in device−/handling-specific VITROCELL® Cloud12 performance (*i.e.*, DF) are unclear, but

are likely due to differences in nebulizer performance, device handling (albeit all partners have used the same SOP), and/or uncertainties in dosimetry methods, *i.e.,* fluorescence spectrometry and QCM. Regardless of these differences and potential particle-related complications, the QCM proved to be a good tool for real-time determination of the transwell insert-delivered material if blank correction is included.

In summary, the following critical steps have been identified, *i.e.* (i) preparation of a stable particle suspension, (ii) nebulization process and output rate of the nebulizer, and (iii) QCM performance and cleaning. These steps have been addressed in this manuscript and in the SOP with the aim to achieve a comparable (nano)particle deposition on the insert well. The approach to develop a detailed SOP to aerosolize various materials has proven to provide comparable results among different laboratories and will support further hazard assessment of aerosolized materials using lung cell models in future experiments in a reliable manner.

Funding

Partners AMI, RIVM, SU, and BASF SE acknowledge the funding by the PATROLS project, European Union' Horizon 2020 Research and Innovation Programme under grant agreement No: 760813. HMGU has also received funding from the European Union Horizon 2020 research and innovation program under grant agreement No. 953183 (HARMLESS project). Anne Bannuscher, Barbara Drasler, Alain Rohrbasser, Alke Petri-Fink and Barbara Rothen-Rutishauser also acknowledge the support by the Adolphe Merkle Foundation. Johanna Samulin Erdem and Shanbeh Zienolddiny acknowledge the support by the National Institute of Occupational Health, Norway. STAMI would like to acknowledge the work of Oda Haarr Foss for excellent technical assistance.

Author statement

Barbara Birk, Manuel Rissel, Robert Landsiedel are employees of BASF. BASF produces some of the test material. In the future, this set-up (Cloud12) might also be used for toxicological testing of BASF products. Otmar Schmid is an employee of the Helmholtz Center Munich, which receives license fees for the VITROCELL® Cloud technology. Otmar Schmid, a co-patent holder of the underlying ALICE Cloud technology, receives a share of these license fees. All other authors declare no competing financial interests.

CRediT authorship contribution statement

Anne Bannuscher: Project administration, Investigation, Methodology, Validation, Data curation, Supervision, Writing – original draft, Writing – review & editing. **Otmar Schmid:** Methodology, Data curation, Writing – review & editing. **Barbara Drasler:** Investigation, Writing – review & editing. **Alain Rohrbasser:** Investigation, Data curation. **Hedwig M. Braakhuis:** Conceptualization, Methodology, Validation, Supervision, Writing – review & editing. **Kirsty Meldrum:** Investigation, Methodology, Validation, Writing – review & editing. **Edwin P. Zwart:** Investigation, Methodology, Validation. **Eric R. Gremmer:** Investigation, Methodology, Validation. **Barbara Birk:** Conceptualization, Methodology, Validation, Writing – review & editing. **Manuel Rissel:** Investigation, Methodology, Validation, Writing – review & editing. **Robert Landsiedel:** Supervision, Funding acquisition, Writing – review & editing. **Elisa Moschini:** Investigation, Methodology, Validation, Writing – review & editing. **Stephen J. Evans:** Methodology, Writing – review & editing. **Pramod Kumar:** Investigation, Methodology, Validation. **Sezer Orak:** Investigation, Methodology, Validation. **Ali Doryab:** Data curation, Writing – review & editing. **Johanna Samulin Erdem:** Investigation, Methodology, Validation, Writing – review & editing. **Rob J. Vandebriel:** Conceptualization, Methodology, Validation, Supervision, Writing – review & editing. **Flemming R. Cassee:** Project administration, Funding acquisition, Writing – review & editing. **Shareen H. Doak:** Project administration, Funding acquisition, Writing – review & editing. **Alke Petri-Fink:** Supervision, Writing – review & editing. **Shanbeh Zienolddiny:** Supervision, Writing – review & editing. **Martin J.D. Clift:** Conceptualization, Methodology, Validation, Supervision, Project administration, Writing – review & editing. **Barbara Rothen-Rutishauser:** Conceptualization, Methodology, Validation, Supervision, Project administration, Funding acquisition, Writing – review & editing.

Declaration of Competing Interest

The authors declare the following financial interests/personal relationships which may be considered as potential competing interests:

Barbara Birk, Manuel Rissel, Robert Landsiedel are employees of BASF. BASF produces some of the test material. In the future this set-up (Cloud12) might be used also for toxicological testing of BASF products. Otmar Schmid is employee of the Helmholtz Zentrum Munich, which receives license fees for the VITROCELL Cloud technology. Otmar Schmid as co-patent holder of the underlying ALICE Cloud technology receives a share of these license fees. All other authors declare no competing financial interests.

Data availability

Data will be made available on request.

Acknowledgments

We gratefully acknowledge the support by VITROCELL® Systems (Germany) for information and advice related to technical details and handling of the VITROCELL® Cloud 12 system and support with an excel sheet for calculation of the deposition factor from the fluorescein data. We thank Sandeep Keshavan, Sandor Balog and Maria Porteiro Figueiras from AMI for the dynamic light scattering measurements.

Appendix A. Supplementary data

Supplementary data to this article can be found online at https://doi.org/10.1016/j.impact.2022.100439.

References

Abubakar, I.I., Tillmann, T., Banerjee, A., 2015. Global, regional, and national age-sex specific all-cause and cause-specific mortality for 240 causes of death, 1990-2013: a systematic analysis for the Global Burden of Disease Study 2013. Lancet. 385 (9963), 117–171.

Arts, J.H.E., Hadi, M., Irfan, M.-A., Keene, A.M., Kreiling, R., Lyon, D., et al., 2015. A decision-making framework for the grouping and testing of nanomaterials (DF4nanoGrouping). Regul. Toxicol. Pharmacol. 71 (2 Supplement), S1–S27.

Arts, J.H.E., Irfan, M.-A., Keene, A.M., Kreiling, R., Lyon, D., Maier, M., et al., 2016. Case studies putting the decision-making framework for the grouping and testing of nanomaterials (DF4nanoGrouping) into practice. Regul. Toxicol. Pharmacol. 76, 234–261.

Aufderheide, M., Mohr, U., 2000. CULTEX–an alternative technique for cultivation and exposure of cells of the respiratory tract to airborne pollutants at the air/liquid interface. Exp. Toxicol. Pathol. 52 (3), 265–270.

Bannuscher, A., Hellack, B., Bahl, A., Laloy, J., Herman, H., Stan, M.S., et al., 2020. Metabolomics profiling to investigate nanomaterial toxicity in vitro and in vivo. Nanotoxicology. 14 (6), 807–826.

Barosova, H., Maione, A.G., Septiadi, D., Sharma, M., Haeni, L., Balog, S., et al., 2020. Use of EpiAlveolar lung model to predict fibrotic potential of multiwalled carbon nanotubes. ACS Nano 14 (4), 3941–3956.

Barosova, H., Meldrum, K., Karakocak, B.B., Balog, S., Doak, S.H., Petri-Fink, A., et al., 2021. Inter-laboratory variability of A549 epithelial cells grown under submerged and air-liquid interface conditions. Toxicol. in Vitro 75, 105178.

Bas, A., Burns, N., Gulotta, A., Junker, J., Drasler, B., Lehner, R., et al., 2021. Understanding the development, standardization, and validation process of alternative in vitro test methods for regulatory approval from a researcher perspective. Small. 17 (15), e2006027.

Bitterle, E., Karg, E., Schroeppel, A., Kreyling, W.G., Tippe, A., Ferron, G.A., et al., 2006. Dose-controlled exposure of A549 epithelial cells at the air-liquid interface to airborne ultrafine carbonaceous particles. Chemosphere. 65 (10), 1784–1790.

Booth, A., Jensen, K.A.. NANoREG D4.12 SOP Probe Sonicator Calibration for Ecotoxicological Testing. Available online: https://www.rivm.nl/en/documenten/nanoreg-d412-sop-probe-sonicator-calibration-for-ecotoxicological-testing.
de Bruijne, K., Ebersviller, S., Sexton, K.G., Lake, S., Leith, D., Goodman, R., et al., 2009. Design and testing of electrostatic aerosol in vitro exposure system (EAVES): an alternative exposure system for particles. Inhal. Toxicol. 21 (2), 91–101.
Ding, Y., Weindl, P., Lenz, A.G., Mayer, P., Krebs, T., Schmid, O., 2020. Quartz crystal microbalances (QCM) are suitable for real-time dosimetry in nanotoxicological studies using VITROCELL(R)Cloud cell exposure systems. Part Fibre Toxicol. 17 (1), 44.
Doryab, A., Taskin, M.B., Stahlhut, P., Schroppel, A., Orak, S., Voss, C., et al., 2021. A Bioinspired in vitro lung model to study particokinetics of nano−/microparticles under cyclic stretch and air-liquid interface conditions. Front. Bioeng. Biotechnol. 9, 616830.
Driessen, M.D., Mues, S., Vennemann, A., Hellack, B., Bannuscher, A., Vimalakanthan, V., et al., 2015. Proteomic analysis of protein carbonylation: a useful tool to unravel nanoparticle toxicity mechanisms. Particle Fibre Toxicol. 12 (1), 36.
Ehrmann, S., Schmid, O., Darquenne, C., Rothen-Rutishauser, B., Sznitman, J., Yang, L., et al., 2020. Innovative preclinical models for pulmonary drug delivery research. Expert Opin. Drug Deliv. 17 (4), 463–478.
Elberskirch, L., Sofranko, A., Liebing, J., Riefler, N., Binder, K., Bonatto Minella, C., et al., 2022. How structured metadata acquisition contributes to the reproducibility of nanosafety studies: evaluation by a round-robin test. Nanomaterials (Basel). 12 (7).
Elliott, J.T., Rösslein, M., Song, N.W., Toman, B., Kinsner- Ovaskainen, A., Maniratanachote, R., et al., 2017. Toward achieving harmonization in a nanocytotoxicity assay measurement through an interlaboratory comparison study. ALTEX – Altern. Anim. Experiment. 34 (2), 201–218.
Endes, C., Schmid, O., Kinnear, C., Mueller, S., Espinosa, S., Vanhecke, D., et al., 2014. An in vitro testing strategy towards mimicking the inhalation of high aspect ratio nanoparticles. Part FibreToxicol. 11 (1), 40.
Fizeşan, I., Cambier, S., Moschini, E., Chary, A., Nelissen, I., Ziebel, J., et al., 2019. In vitro exposure of a 3D-tetraculture representative for the alveolar barrier at the air-liquid interface to silver particles and nanowires. Particle Fibre Toxicol. 16 (1), 14.
Hartung, T., Bremer, S., Casati, S., Coecke, S., Corvi, R., Fortaner, S., et al., 2004. A modular approach to the ECVAM principles on test validity. Altern. Lab. Anim 32 (5), 467–472.
Hiemstra, P.S., Grootaers, G., van der Does, A.M., Krul, C.A.M., Kooter, I.M., 2018. Human lung epithelial cell cultures for analysis of inhaled toxicants: lessons learned and future directions. Toxicol. in Vitro 47, 137–146.
Ji, J., Upadhyay, S., Xiong, X., Malmlöf, M., Sandström, T., Gerde, P., et al., 2018. Multi-cellular human bronchial models exposed to diesel exhaust particles: assessment of inflammation, oxidative stress and macrophage polarization. Particle Fibre Toxicol. 15 (1), 19.
Karkossa, I., Bannuscher, A., Hellack, B., Bahl, A., Buhs, S., Nollau, P., et al., 2019. An in-depth multi-omics analysis in RLE-6TN rat alveolar epithelial cells allows for nanomaterial categorization. Part Fibre Toxicol. 16 (1), 38.
Keiji Kanazawa, K., Gordon, J.G., 1985. The oscillation frequency of a quartz resonator in contact with liquid. Anal. Chim. Acta 175, 99–105.
Lacroix, G., Koch, W., Ritter, D., Gutleb, A.C., Larsen, S.T., Loret, T., et al., 2018. Air-liquid interface in vitro models for respiratory toxicology research: consensus workshop and recommendations. Appl In Vitro Tox. 4 (2), 91–106.
Lenz, A.G., Karg, E., Lentner, B., Dittrich, V., Brandenberger, C., Rothen-Rutishauser, B., et al., 2009. A dose-controlled system for air-liquid interface cell exposure and its application to zinc oxide nanoparticles. Part Fibre Toxicol. 6 (1), 32.
Lenz, A.G., Stoeger, T., Cei, D., Schmidmeir, M., Semren, N., Burgstaller, G., et al., 2014. Efficient bioactive delivery of aerosolized drugs to human pulmonary epithelial cells cultured in air-liquid interface conditions. Am. J. Respir. Cell Mol. Biol. 51 (4), 526–535.
Limbach, L.K., Li, Y., Grass, R.N., Brunner, T.J., Hintermann, M.A., Muller, M., et al., 2005. Oxide nanoparticle uptake in human lung fibroblasts: effects of particle size, agglomeration, and diffusion at low concentrations. Environ. Sci. Technol. 39 (23), 9370–9376.
Lynch, I., Cedervall, T., Lundqvist, M., Cabaleiro-Lago, C., Linse, S., Dawson, K.A., 2007. The nanoparticle-protein complex as a biological entity; a complex fluids and surface science challenge for the 21st century. Adv. Colloid Interf. Sci. 134-135, 167–174.
OECD, 2018. Guidance Document on Good In Vitro Method Practices (GIVIMP). OECD Publishing, Paris.
Ortelli, S., Costa, A.L., Zanoni, I., Blosi, M., Geiss, O., Bianchi, I., et al., 2021. TiO2@BSA nano-composites investigated through orthogonal multi-techniques characterization platform. Colloids Surf. B: Biointerfaces 207, 112037.
Paur, H.R., Cassee, F.R., Teeguarden, J.G., Fissan, H., Diabate, S., Aufderheide, M., et al., 2011. In-vitro cell exposure studies for the assessment of nanoparticle toxicity in the lung-A dialog between aerosol science and biology. J. Aerosol Sci. 42, 668–692.
Petersen, E.J., Reipa, V., Xia, M., Sharma, M., 2021. Resources for developing reliable and reproducible in vitro toxicological test methods. Chem. Res. Toxicol. 34 (6), 1367–1369.
Ritter, D., Knebel, J., Niehof, M., Loinaz, I., Marradi, M., Gracia, R., et al., 2020. In vitro inhalation cytotoxicity testing of therapeutic nanosystems for pulmonary infection. Toxicol. in Vitro 63, 104714.
Robock, K., 1973. Standard quartz DQ12 < 5 μm For experimental pneumoconiosis research projects in the federal republic of germany. Ann. Occup. Hyg. 16 (1), 63–66.
Röhm, M., Carle, S., Maigler, F., Flamm, J., Kramer, V., Mavoungou, C., et al., 2017. A comprehensive screening platform for aerosolizable protein formulations for intranasal and pulmonary drug delivery. Int. J. Pharm. 532 (1), 537–546.
Savi, M., Kalberer, M., Lang, D., Ryser, M., Fierz, M., Gaschen, A., et al., 2008. A novel exposure system for the efficient and controlled deposition of aerosol particles onto cell cultures. Environ. Sci. Technol. 42 (15), 5667–5674.
Schmid, O., Cassee, F.R., 2017. On the pivotal role of dose for particle toxicology and risk assessment: exposure is a poor surrogate for delivered dose. Part FibreToxicol. 14 (1), 52.
Schmid, O., Jud, C., Umehara, Y., Mueller, D., Bucholski, A., Gruber, F., et al., 2017. Biokinetics of aerosolized liposomal ciclosporin a in human lung cells in vitro using an air-liquid cell interface exposure system. J. Aerosol. Med. Pulm. Drug. Deliv. 30 (6), 411–424.
Upadhyay, S., Palmberg, L., 2018. Air-liquid interface: relevant in vitro models for investigating air pollutant-induced pulmonary toxicity. Toxicol. Sci. 164 (1), 21–30.
Voisin, C., Aerts, C., Jakubczk, E., Tonnel, A.B., 1977. La culture cellulaire en phase gazeuse. Un nouveau modele experimental d'etude in vitro des activites des macrophages alveolaires. Bull. Eur. Physiopathol. Respir. 13 (1), 69–82.
Wiemann, M., Vennemann, A., Sauer, U.G., Wiench, K., Ma-Hock, L., Landsiedel, R., 2016. An in vitro alveolar macrophage assay for predicting the short-term inhalation toxicity of nanomaterials. J. Nanobiotechnol. 14 (1), 16.
Wohlleben, W., Driessen, M.D., Raesch, S., Schaefer, U.F., Schulze, C., Vacano, B., et al., 2016. Influence of agglomeration and specific lung lining lipid/protein interaction on short-term inhalation toxicity. Nanotoxicology. 10 (7), 970–980.
Xia, T., Hamilton, R.F., Bonner, J.C., Crandall, E.D., Elder, A., Fazlollahi, F., et al., 2013. Interlaboratory evaluation of *in vitro* cytotoxicity and inflammatory responses to engineered nanomaterials: The NIEHS nano GO consortium. Environ. Health Perspect. 121 (6), 683–690.